RSC Advances

ROYAL SOCIETY OF CHEMISTRY

www.rsc.org/advances

Effect of the resorcin[4]arene host on the catalytic epoxidation of Mn(III)-based resorcin[4]arene–metalloporphyrin conjugate

Talal F. Al-Azemi* and Mickey Vinodh

[a]*Department of Chemistry, Kuwait University, P O Box 5969, Safat 13060, Kuwait.* *Corresponding author. Tel.: +965-2498-5540; fax: +965-2481-6482; e-mail: t.alazemi@ku.edu.kw

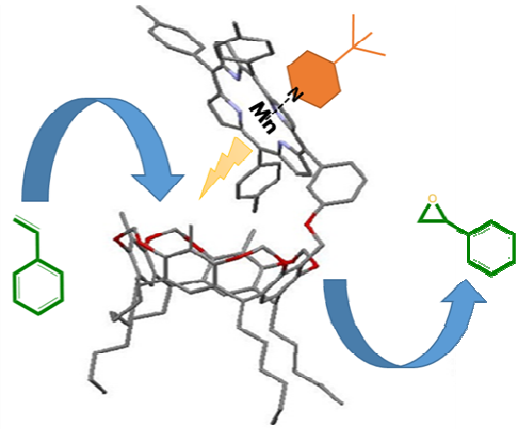

RSC Advances

PAPER

Effect of the resorcin[4]arene host on the catalytic epoxidation of Mn(III)-based resorcin[4]arene–metalloporphyrin conjugate

Received 0th January 2015,
Accepted 00th Month 20xx

DOI: 10.1039/x0xx00000x

www.rsc.org/advances

Talal F. Al-Azemi* and Mickey Vinodh

The single-crystal X-ray diffraction data, binding behavior, and epoxidation reactions of the cavitand resorcin[4]arene–porphyrin conjugate are presented. Polar and nonpolar organic molecules such as pyridine or styrene were included in the cavity of resorcin[4]arene to form a 1:1 complex in the solid state, as demonstrated by single-crystal X-ray diffraction analysis. Binding studies revealed that the presence of resorcin[4]arene enhanced the association constant, obtained from UV titration, by 50% compared to the original porphyrin. The epoxidation of the reaction of alkenes with the Mn(III)-based resorcin[4]arene–porphyrin conjugate showed enhanced activity and depended on the olefins and axial ligands used.

Introduction

Metalloporphyrin-based supramolecular architectures have gained considerable attention for their stabilities and ability to increase catalytic activities.[1–2] Functional materials comprising metalloporphyrins and macrocyclic cavitands such as cyclodextrins,[3–4] calixarenes,[5–7] and resorcinarenes [8–10] are attractive model systems. The combination of the well-known catalytic efficiency of metalloporphyrins with the receptor characteristics of these cavitands has been shown to provide synergistic advantages in the stability, reactivity, and selectivity of the porphyrin fragments.[5–10]

The success of a macrocyclic receptor depends on its guest inclusion capabilities to ensure strong and precise molecular recognition. On the other hand, epoxides are versatile intermediates in organic synthesis. In natural systems, alkene epoxidation occurs through the enzymatic action of cytochrome P450.[9] Synthetic models, especially Mn(III)–porphyrins have been extensively investigated as catalysts for alkene epoxidations.[11–13] In the presence of an oxygen donor and an activating axial ligand, it is reported that a Mn(V)=O species first forms in the Mn(III)-catalyzed epoxidation, which then transfers its oxygen to the alkene substrate to form the epoxide. Many of these model systems utilize Mn(III)–porphyrins that are functionalized with straps or caps to establish an environment in which the oxygen transfer from the metal to the substrate is under steric control, resulting in enhanced reaction rates and selectivity. For example, regio- and stereo-selective oxidation has been achieved, in which *cis*-stilbene is oxidized with a major preference for the production of the *cis*-epoxide.[13(d)]

Appropriate structural modifications of the receptor entity are always necessary to tune the special features of guest encapsulation and reactivity. Although, there are many examples in the literature of the synthesis of resorcinarene–porphyrin conjugates and their use in guest complexation, the use of Mn(III)–resorcinarene–porphyrin conjugates as a catalyst in alkene epoxidation reactions has not been reported. We have previously reported the synthesis of the resorcin[4]arene–porphyrin conjugate and the effect of resorcin[4]arene (RC) on the quenching behavior of the porphyrin fragment (Scheme 1).[14] In this work, we report single-crystal X-ray diffraction studies of the resorcin[4]arene–porphyrin conjugate (RCP) and the inclusion of polar and nonpolar organic molecules in the solid state. The effects of the shape and size of the cavity on the substrate and the axial-ligand binding behavior of the conjugate were studied in detail and will be discussed. The catalytic epoxidation of Mn(III)-based resorcin[4]arene–metalloporphyrin and the size dependence of the encapsulation ability of the resorcin[4]arene conjugate in the epoxidation reactions of alkene is also reported.

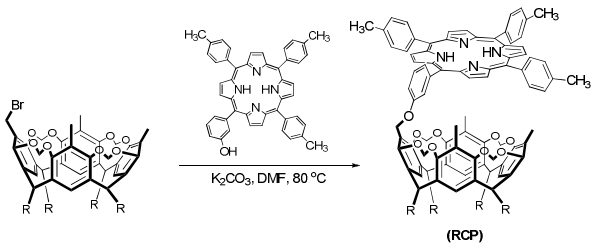

Scheme 1 Synthesis of the cavitand resorcin[4]arene–porphyrin conjugate (RCP).

Department of Chemistry, Kuwait University, PO Box 5969, Safat 13060, Kuwait. E-mail: t.alazemi@ku.edu.kw; Tel.: +965-2498-5540; Fax: +965-2481-6482.
† Footnotes relating to the title and/or authors should appear here.
Electronic Supplementary Information (ESI) available: [details of any supplementary information available should be included here]. See DOI: 10.1039/x0xx00000x

Experimental Section

The synthesis and characterization of cavitand RC and their porphyrin-appended analogue, RCP, along with the zinc-based metal derivative, were prepared according to previously reported procedures (see supporting information).[14]

Characterization

Ultraviolet–visible (UV–vis) spectra were recorded on a UV–vis spectrophotometer (Varian Cary 5, Agilent, USA). Fast atom bombardment (FAB) mass analysis was performed using a mass spectrometer (DFS High Resolution GC/MS, Thermo Scientific, USA). Proton nuclear magnetic resonance (^{1}H NMR) spectroscopy was performed using two spectrometers (Avance II, 600 MHz, Bruker, Germany; DPX 400, 400 MHz, Bruker, Germany). All single-crystal X-ray diffraction data were collected on a diffractometer (R-AXIS RAPID, Rigaku, Japan) using filtered Mo K_α radiation. The data were collected at a temperature of -123 °C (Oxford Cryosystems, UK). The structure was solved by direct methods and expanded using Fourier analysis. The non-hydrogen atoms were refined anisotropically; the hydrogen atoms were refined using the riding model. Gas chromatography (GC) analysis was performed on a gas chromatograph (GC-2010, Shimadzu GC-2010, Japan) with a flame ionization detector (FID) detector using a chiral capillary column (length: 30 m, ID: 0.25 mm) (Supelco β-Dex 225, Sigma-Aldrich, USA). Flash column chromatography was performed using sukuca gek (Silica gel 60, 230–400 mesh ASTM, EMD Millipore, Merck KGaA, Germany). All other reagents and solvents were of reagent-grade purity and used without further purification.

Synthesis manganese derivatives of RCP

Manganese derivative of porphyrin Resorcin[4]arene conjugate (Mn(III)RCP). RCP (200 mg) was dissolved in a chloroform–methanol mixture (2:1 v/v, 50 mL). $Mn(OAc)_2$ (200 Mg) added to the solution and refluxed for 5 h. When the metal insertion was complete (indicated by the disappearance of the 650-nm peak in the UV–vis spectrum), the solvent was evaporated. The residue was extracted with dichloromethane (50 mL) and washed with water 3–4 times to remove unreacted manganese salt. The porphyrin solution was then dried and dissolved in chloroform (50 mL). A saturated NaCl solution (100 mL) was added to this solution and stirred at room temperature for 8 h. The water layer was then removed and the chloroform was evaporated. The crude material was dissolved in dichloromethane (50 mL) and washed several times with water. The solvent was finally removed under reduced temperature and the product was dried under vacuum until a constant weight was obtained (>90% yield). UV–vis spectrum recorded in CH_2Cl_2, λ_{max} (nm) ($\varepsilon \times 10^{-5}$ M^{-1} cm^{-1}): 377 (0.58), 402 (0.49), 479 (1.14), 586 (0.10) and 622 (0.13). FAB mass: 1653 [M-Cl].

Single crystal X-ray diffraction analysis

Singles crystals of RC and RCP that were suitable for single-crystal X-ray diffraction were grown from the solvent diffusion method using ethyl acetate and hexane. The single-crystal data were collected on a diffractometer (R-AXIS RAPID, Rigaku, Japan) diffractometer using Rigaku's Crystalclear software package at -123 °C. The structure was solved and refined using the Bruker SHELXTL Software Package (structure solution program: SHELXS-97; refinement program: SHELXL-97). The crystallographic data for the structures reported in this paper have been deposited at the Cambridge Crystallographic Data Centre as supplementary publications (CCDC 958843–958847. Copies of the data can be obtained, free of charge, upon submission of application to CCDC, 12 Union Road, Cambridge CB2 1EZ, UK (fax: +44(0) 1223 336033 or e-mail: deposit@ccdc.cam.ac.uk).

UV–vis titrations

A 25-mL sample of the porphyrins solution was prepared at a concentration of 8 μM in spectroscopic-grade solvent (chloroform was dried over calcium chloride and neutral alumina). A 10-mL sample of the ligand solution was prepared at a concentration of 0.004–0.2 M in a spectroscopic-grade solvent. All titration experiments were carried out with 5 mL of a receptor solution in a quartz cell at 298 K, and UV–vis spectra were recorded upon successive addition of aliquots of the stock solution of the appropriate ligands with a microsyringe. The UV–vis absorbance at three different wavelengths was fitted to a 1:1 binding isotherm by nonlinear least-squares treatment using Microsoft Excel to determine the association constant, K_a.[15]

Epoxidation reaction-procedure

The epoxidation studies of the catalyst systems, cavitand Mn-based RCP (MnRCP) and Mn–tetratolylporphyrin (MnTTP), were carried out simultaneously for each set of substrate–ligand combination. Under typical reaction conditions, the catalyst (0.5 μmol) dissolved in dichloromethane (2 mL) in a 10-mL round bottom flask. The axial pyridine ligand (200 μmol) was added to the solution and stirred slowly for 5 min. Styrene (500 μmol) was then added and the solution was stirred again for another 5 min. The phase-transfer regent (T-butyl ammonium iodide, 35 μmol) was added to this system followed by the addition of sodium hypochlorite solution (0.6 M, 2 mL). The reaction mixture was stirred at room temperature, and at predetermined intervals, a small aliquant (200 μL) was withdrawn from the organic phase and passed through a small silica gel column (length: 1 cm; diameter: 5 mm) and eluted with dichloromethane (1 mL). The dichloromethane was dried over Na_2SO_4 and removed by filtration. Finally, 1 μL of the eluted CH_2Cl_2 was injected into the GC column to determine the progress of the reaction.

Results and Discussion

Crystallography: crystal structure of resorcin[4]arene host with small guest molecules

Resorcin[4]arenes are well known for their ability to encapsulate small organic and cationic species.[16–17] The porphyrin unit is attached to the cavitand resorcin[4]arene moiety through a methyl ether linkage. Such a spacer is expected to provide sufficient flexibility to the porphyrin unit to orient at a stable low-energy position with respect to RC. Single crystals of RCP that were suitable for X-ray diffraction were obtained by controlled solvent evaporation of RCP dissolved in ethyl acetate. The crystal structure of RCP obtained from the XRD data is depicted in Fig. 1. The crystal network was found to contain one solvent ethyl acetate molecule per RCP molecule, occupying the void between porphyrin and resorcinarene. The molecular structure obtained from the crystal data demonstrates the orientation of the porphyrin unit over the RC cavity in the solid state.

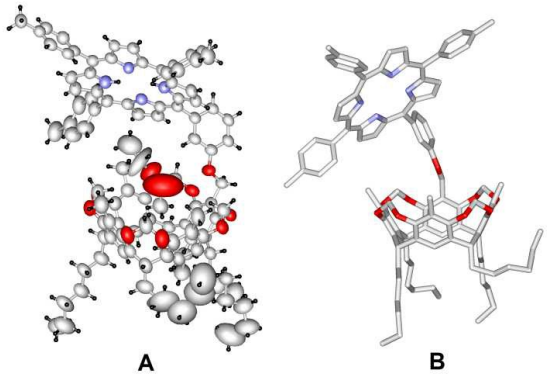

Fig. 1 Molecular structure of RCP derived from single-crystal X-ray diffraction data: (a) thermal ellipsoid representation (50% probability); (b) capped-sticks representation in which the hydrogen atoms and the trapped ethyl acetate moiety are hidden for clarity. Color code: red – oxygen, blue – nitrogen, gray – carbon, black – hydrogen.

The unit cell of the RCP crystal contains two resorcin[4]arene–porphyrin conjugates per cell. As demonstrated in Fig. 2, the RCs in each unit cell are occupied in diagonal positions and the porphyrins are intercalated at the center. The three-dimensional packing of the RCP crystal is arranged in a zigzag fashion, with alternate species inverted from each other (see ESI).

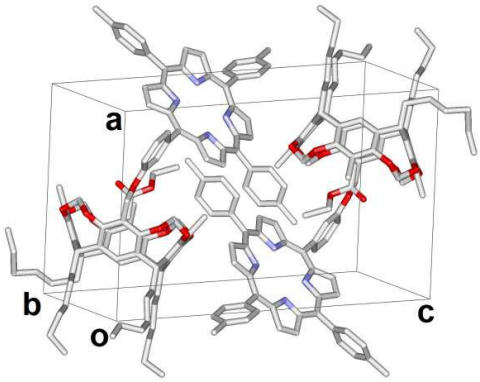

Fig. 2 Unit cell of RCP crystals (color code: red – oxygen, gray- carbon; the hydrogen atoms are hidden for clarity).

Because of the difficulty associated with obtaining the RCP crystal structure by single-crystal X-ray diffraction analysis, and in order to demonstrate the ability of RC to accommodate small organic molecules, a bowl-shaped rigid RC was co-crystallized with styrene and pyridine. The X-ray crystal structure of the crown-like structure of the bridged cavitand methyleneoxy resorcin[4]arene is shown in Fig. 3. The top most diameter of the rigid bowl is about 8.8 Å and that of the lower end is about 5.6 Å, which is suitable for accommodating small organic molecules or ions. The aliphatic heptyl chains extend downwards and are slightly disordered at the tail ends owing to the thermal motions (Fig. 3).

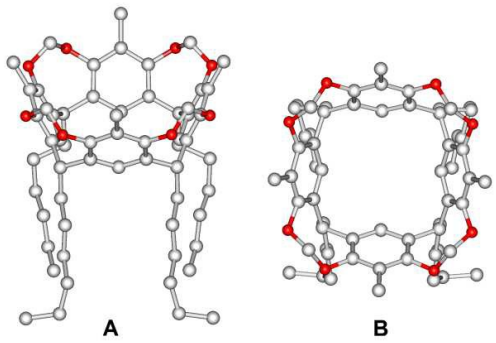

Fig. 3 Structure of resorcinarene framework from the crystal data of resorcin[4]arene–styrene (RCSTY); the styrene and all hydrogen atoms are hidden to show the structure more clearly: (a) side view; (b) top view. Color code: red – oxygen, gray – carbon.

Crystals of the inclusion compounds were obtained by co-crystallizing saturated solutions of the host (resorcin[4]arene) with the respective guests (pyridine or styrene). The saturated solutions were prepared by dissolving the host in a warm solvent (guest, at 70 °C) under gentle stirring. The solutions were slowly cooled and evaporated, allowing the inclusion compounds to crystallize. The inclusion complexes of RC with pyridine (RCPY) and styrene (RCSTY), derived from XRD data, are depicted in Fig. 4. Even if their physical shape and size in the crystalline state are different, the crysatllographic space

group of both RCPY and RCSTY were observed to be the same and the unit cell parameters are almost similar.

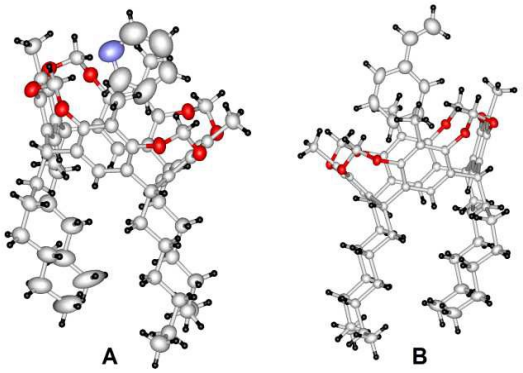

Fig. 4 Thermal ellipsoid representation of the crystal structure of (a) resorcin[4]arene–pyridine (RCPY) and (b) resorcin[4]arene–styrene (RCSTY). Color code: red – oxygen, blue – nitrogen, gray – carbon, black – hydrogen.

Single-crystal X-ray diffraction studies have shown that the terminal double bond of styrene and the nitrogen atom of pyridine are outside the cavity of the host molecule. In a host–guest environment, the ease with which these guest molecules fit inside the host molecules as well as the availability of their reactive functional sites to engage in chemical reactions are very important attributes of efficient guest molecules. Such encapsulation characteristics could be easily demonstrated in the solid state by the single-crystal X-ray diffraction technique.

.

Binding studies

Encouraged by results of the study on the crystal structure, which showed the ability of cavitand RC to accommodate polar and nonpolar neutral molecules such as pyridine and styrene, the Zn(II)-based resorcin[4]arene–metalloporphyrin conjugate (Zn(II)RCP) was prepared quantitatively from the reaction of free base porphyrin with excess $Zn(OAc)_2$ in $CHCl_3$. Zn–porphyrin is known to bind only one axial ligand, resulting in a five-coordinated zinc atom.[18] In order to demonstrate the ability of Zn(II)RCP to incorporate pyridine into the cavity in a solution, binding studies were performed in $CHCl_3$ with pyridine derivatives using UV titration. For comparison, analogous experiments with Zn–tetratolylporphyrin (ZnTTP) were also performed.

In Fig. 5a, the absorption spectra of ZnRCP in chloroform exhibit transitions that are characteristic of Zn(II)–porphyrins. Specifically, a symmetry-permitted transition centered at 424 nm corresponding to the Soret band, as well as a transition at 550 nm (Q band) are clearly visible. The addition of pyridine or 4-*tert*–butylpyridine resulted in hyperchromic shifts in the absorption spectra: a new Soret band appears at 430 nm and two Q bands appear at 563 and 603 nm. A typical example of UV titration is shown in Fig. 5b.

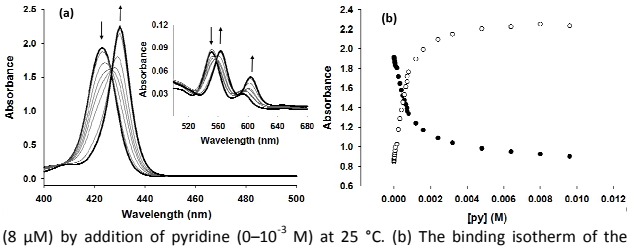

(8 μM) by addition of pyridine (0–10^{-3} M) at 25 °C. (b) The binding isotherm of the ZnRCP–pyridine system at 424 nm (●) and 430 nm (○).

To characterize the effect of the RC conjugate on the binding affinity of Zn(II)RCP, UV–vis titration experiments of Zn(II)RCP and ZnTTP with pyridine and 4-*tert*-butylpyridine as guests were performed in chloroform. The data fitted well to a 1:1 binding isotherm and the binding constant was determined from nonlinear least-square fitting,[15] using the change in the absorbance at 430 nm; the results are summarized in Table 1. The calculated association constant of ZnTTP (1.06×10^3 M^{-1}) is similar to that calculated for Zn–tetraphenylporphyrin (ZnTPP) by UV titration.[13c,17] On the other hand, the calculated K_a of Zn(II)RCP in chloroform is 1.54×10^3 M^{-1}, which is approximately 50% higher than that of ZnTTP. Similarly, titration of ZnRCP with 4-*tert*–butylpyridine, gave $K_a = 1.46 \times 10^3$ M^{-1}, which is slightly lower than K_a of ZnTTP. From the UV–vis titration experiment, it is evident that the increase in K_a of ZnRCP bound to pyridine was due to the favorable encapsulation of the axial ligand (pyridine) stabilized by the π-wall of the resorcinarene conjugate host. In contrast, the bulky substituent in 4-*tert*–butylpyridine prevented the accommodation inside the RC cavity, and the guest was thus bound to Zn–porphyrin from the opposite side of RC. The results of the binding study are in agreement with single-crystal X-ray data. In particular, the free rotation of the ether linkage in RCP exhibited lower binding affinity than the highly rigid cavities of cap-or-clip porphyrins reported in the literature.[5,13c]

Table 1 Association Constants, $K_a(M^{-1})$, for the formation of 1:1 complexes measured by UV–vis titration in $CHCl_3$ at 298 K (with percentage error).[a]

Entry	Porphyrin	Ligand	K_a (M^{-1})
1	ZnTTP	Pyridine	1.06×10^3 (5%)
2		4-*tert*-butylpyridine	1.67×10^3 (3%)
3	ZnRCP	Pyridine	1.54×10^3 (6%)
4		4-*tert*-butylpyridine	1.41×10^3 (5%)

[a] The titration data was fitted to the 1:1 binding model, error < 8%. [a]K_a was measured from the change in absorbance at 430 nm.

Epoxidation reactions

It is well-known that a manganese porphyrin catalyzes epoxidation of styrene in the presence of an oxygen source, and the rate of product formation is greatly increased by the presence of pyridine. The role of pyridine is to coordinate to the axial position of Mn–porphyrin and thereby facilitate the formation of Mn(V)–oxo species,[11–13] which is essential for

epoxidation reactions. The Mn(III)-based resorcin[4]arene–metalloporphyrin conjugate (Mn(III)RCP) was prepared from the reaction of the free base porphyrin core of RCP with $Mn(OAc)_2$ in a chloroform–methanol mixture, followed by treatment with saturated NaCl. Based on the single-crystal XRD analysis of RCP and the ability of cavitand RC to encapsulate guest substrates such as pyridine and styrene inside the cavity and the favorable orientation of functional groups over the resorcinarene moiety in the crystal network, in addition, the result obtained from the binding studies. Different olefin and axial ligand combinations—styrene:t-butylpyridine, t-butylstyrene:pyridine, and t-butylstyrene:t-butylpyridine—were used to study the effect of the RC cavity in the epoxidation reaction of Mn(III)RCP. Similarly, in the investigation of epoxidation reactions, Mn(III)–tetratolylporphyrin (MnTTP) was prepared and epoxidation experiments were conducted for comparison. The combinations of substrate and axial ligand utilized in the MnRCP-catalyzed epoxidation reactions are depicted in Fig. 6.

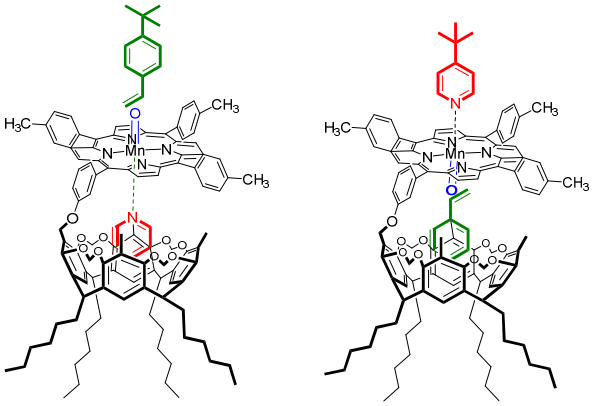

Fig. 6 Representation of the combinations of substrate and axial ligand utilized in the MnRCP-catalyzed epoxidation reactions: (a) Pyridine–4-*tert*-butylstyrene; (b) 4-*tert*-butylpyridine–styrene.

The results of the epoxidation reaction of 4-*tert*-buylstyrene catalyzed by MnRCP and MnTTP in the presence of pyridine as an axial ligand are shown in Fig. 7. At the initial epoxidation rate, the MnRCP-catalyzed conversion of styrene was approximately 10 times higher than that of the MnTTP-catalyzed conversion, which is generally related to the higher binding constant of the axial ligand. The significant variations in epoxidation performance exhibited by MnRCP compared to the unconjugated porphyrin at the initial stages clearly show the role of the cavity in enhancing the catalytic epoxidation (see Fig. 5a). The obtained data are in agreement with the results of single-crystal XRD studies and the binding studies of the ZnRCP analogue, in which the rate enhancing effect was the result of the inclusion of pyridine inside the RC cavity.

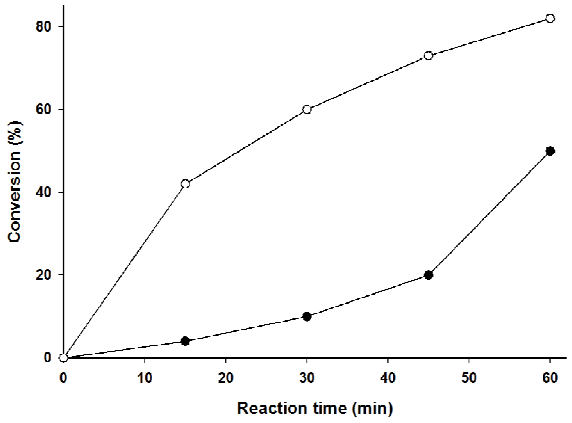

Fig. 7 Plot of conversion (%) as a function of reaction time of the epoxidation reaction of t-butylstyrene catalyzed by MnTTP (●)and MnRCP (○)in the presence of pyridine as an axial ligand.

Using the bulky t-butylpyridine as axial ligand is expected to enable the substrate (styrene) to be encapsulated inside the RC cavity (Fig. 6b). Fig. 8 shows the results of the epoxidation of styrene and 4-*tert*-butylpyridine as the axial ligand catalyzed by MnRCP and MnTTP. In the initial stages, MnRCP showed higher conversion rate than MnTTP, which is an indication of the role of the RC host in the epoxidation reaction. However, the increased activity of MnTTP can be explained in terms of the favorable electronic effects induced by the *tert*-butyl functional groups at the gamma position of pyridine, which increased the coordinating ability of pyridine by increasing the basicity. In the absence of an axial ligand, epoxidation of both styrene and t-butylstyrene was observed to be negligible for these catalyst systems (data not shown).

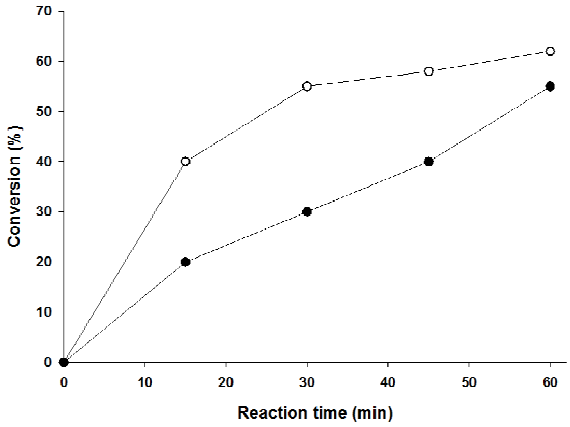

Fig. 8 Plot of conversion (%) as a function of reaction time of the epoxidation reaction of styrene catalyzed by MnTTP (●)and MnRCP (○) in the presence of t-butylpyridine as an axial ligand.

In order to provide better understanding of the role of the RC conjugate in the catalytic performance of MnRCP, a bulky substrate (4-*tert*-butylstyrene) and an axial ligand (4-*tert*-butylpyridine) were used (Fig. 9). MnRCP exhibited lower catalytic activity than the MnTTP, indicating that RC played no role in the epoxidation reaction, and clearly showing the dependence of the conjugate on the size and shape of pyridines or styrenes present in the reaction medium.

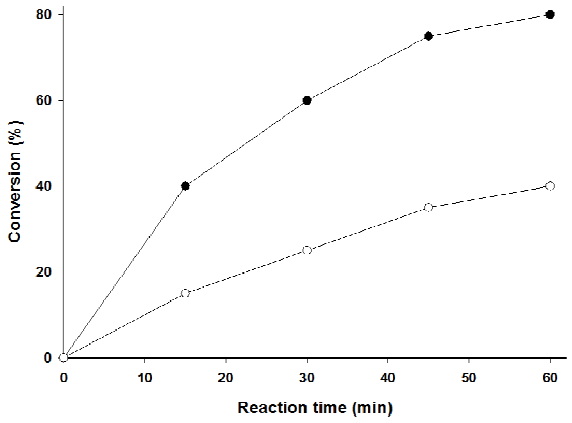

Fig. 9 Plot of percent conversion (%) as a function of reaction time of the epoxidation reaction of t-butylstyrene catalyzed by MnTTP (●)and MnRCP (○)in the presence of t-butylpyridine as an axial ligand.

Even though the analysis of these systems was complicated by the possible competition between the occurrence of the epoxidation reactions inside and outside the RC cavity, the results clearly show that the variations in epoxidation efficiency exhibited by Mn(III)-based resorcinarene–metalloporphyrin conjugates can be correlated with the recognition characteristics of the corresponding RC conjugates towards olefins and pyridines under study.

Conclusions

The results of our research clearly demonstrate the impact of the size and shape of the cavitand resorcin[4]arene on the stability and reactivity of the porphyrin fragment. Single-crystal X-ray diffraction technique studies revealed the formation of an inclusion complex of resorcinarene with pyridine and styrene in the solid state. The binding studies showed that the presence of resorcin[4]arene led to a 50% increase in the association constant of Zn–porphyrin with pyridine as the axial ligand. Because the rigid bowl-shaped cavitand resorcin[4]arene was a batter host for pyridine and styrene, the Mn(III)-based metalloporphyrin system showed higher catalytic efficiency in epoxidation reaction when coordinated with the pyridine axial ligand or encapsulation of styrene inside the cavity of the resorcin[4]arene conjugate. Further studies and modifications of resorcinarene–porphyrin conjugates in terms of the increases in rigidly, stability, and catalytic activity are underway in our laboratories.

Acknowledgements

The support of the University of Kuwait, received through research grant no. SC01/12, and the facilities of ANALAB and SAF (grant no. GS01/01, GS03/01, GS01/03, GS01/05, and GS03/08) are gratefully acknowledged.

Notes and references

‡ Footnotes relating to the main text should appear here. These might include comments relevant to but not central to the matter under discussion, limited experimental and spectral data, and crystallographic data.

[a]*Department of Chemistry, Kuwait University, P O Box 5969, Safat 13060, Kuwait.* ∗Corresponding author. Tel.: +965-2498-5540; fax: +965-2481-6482; e-mail: t.alazemi@ku.edu.kw

1 Y. Ninomiya, M. Kozaki, S. Suzuki andK. Okada, *Bull. Chem. Soc. Jpn.,* 2014, **87**, 1195; N. T. Nguyen, G. M. Mamardashvili,O. M. Kulikova, I. G. Scheblykin,N. Z. Mamardashvili and W. Dehaen, *RCS adv.* 2014, **4**, 19703; C. Li, X. Zhao, X. Gao, Q. Wang and Z. Li, *Chin. J. Chem.,* 2013, **31**, 582; C. B. KC, G. N. Lim, P. A. Karr and F. D'Souza, *Chem. Eur. J.,* 2014, **20**, 7725; N. T. Nguyen, G. M. Mamardashvili, M. Gruzdev, N. Z. Mamardashvili and W. Dehaen, *Supramolecular Chem.,* 2013, **3**, 180.

2 M. Vinodh, F. H. Alipour, A. A. Mohamod and T. F. Al-Azemi, *Molecules,* 2012, **17**, 11763; R. Beletskaya, V. S. Tyurin, A. S. Tsivadze, R. Guilard and C. Stern, *Chem. Rev.,* 2009, **109**, 1659; A. K. Burrell, D. L. Officer, P. G. Plieger and D. C. Reid, *Chem. Rev.,* 2001, **101**, 2751.

3 Y. Kuroda, T. Sera and H. Ogoshi, *J. Am. Chem. Soc.,* 1991, **113**, 2793; R. Breslow, X. Zhang and Y. Huang, *J. Am. Chem. Soc*., 1997, **119**, 4535; L. Weber, R. Hommel, S. J. Behling, G. Haufe and H. Hennig, *J. Am. Chem. Soc.,* 1994,**116**, 2400.

4 A. Puglisi, R. Purrello, E. Rizzarelli, S. Sortino and G. Vecchio, *New J. Chem.,* 2007, **31**, 1499; K. Hosokawa, Y. Miura, T. Kiba, T. Kakuchi and S. F. Sato, *Chem. Lett.,* 2008, **37**, 60; Y. Guo, P. Zhang, J. Chao, S. Shuang and C. Dong, C. *Spectrochim. Acta A*, 2008, **71A**, 946; X.-X. Li, J.-W. Wang, Y.-J. Guo, L.-H. Kongand J.-H. Pan, *J. Incl. Phenom. Macro.,* 2007, **58**, 307.

5 H. Iwamoto, Y. Yukimasa and Y. Fukazawa, *Tetrahedron Lett.,* 2002, **43**, 8191.

6 N. Zh. Mamardashvili and O. I. Koifman, *Russ. J. Gen. Chem.*, 2005, **6**, 787.

7 D. M. Rudkevich, W. Verboom and D. N. Reinhoudt, *J. Org. Chem*., 1995, **60**, 6585.

8 S. D. Starnes, D. M. Rudkevich and J. Rebek, *Org. Lett.*, 2000, **14**, 1995; J. Nakazawa, M. Mizuki, Y. Shimazaki, F. Tani and Y. Naruta, *Org. Lett.*, 2006, **19**, 4275; J. Nakazawa, Y. Sakae, M. Mizuk and Y. Naruta, *J. Org. Chem.* 2007, **72**, 9448; J. Nakazawa, J. Hagiwara, M. Mizuki, Y. Shimazaki, F. Tani and Y. Naruta, *Angew. Chem.,* 2005, **117**, 2810.

9 J. T. Groves and Y. Z. Han in: *Cytochrome P 450: Structure, mechanism and Biochemistry*, ed. P. R. Ortiz de Montellano, Plenum Press, New York, 2nd edn., 1995, 2nd edn., pp. 3–48.

10 D. Fankhauser, D. Kolarski, W. R. Gruning and F. Diederich, *Eur. J. Org. Chem.,* 2014, 17, 3575; B. Botta, P. Ricciardi, C. Galeffi, M. Botta, A. Tafi, R. Pogni, R. Iacovino, I. Garella, I.; B.

Blasio and G. D. Monache, *Org. Biomol. Chem.,* 2003, **1**, 3131.
11 D. Monti, A. Pastorini, G. Mancini, S. Borocci and P. Tagliatesta, J. *Mol. Catal. A: Chemical,* 2002, **179**, 125.
12 V. Pardines and G. Pratvil, *Angew. Chem. Int. Ed.,* 2013, 52, 2185.
13 (a) J. A. Elemans, M. B. Claase, P. P. Aarts, A. E. Rowan, A. P. Schenning and R. J. Nolte, *J. Org. Chem*., 1999, **64**, 7009; J. A. Elemans, E. J. Bijsterveld, A. E. Rowan and R. J. Nolte, *Eur. J. Org. Chem.,* 2007,5,751; (c) J. A. Elemans, E. J. Bijsterveld, A. E. Rowan and R. J. Nolte, *Chem. Commun.*, 2000, 2443; (d) J. A. Elemans, E. J. Bijsterveld, A. E. Rowan and R. J. Nolte, *Nature*, 2003, **424**, 915.
14 T. F. Al-Azemi and M. Vinodh, *Tetrahedron* 2011, **67**, 2585.
15 M. Hong, Y. Zhang and Y. Liu, *J. Org. Chem.,* 2015, **80**, 1849; S. Busi, H. Saxell, R. Frohlich and K. Rissanen, *Cryst, Eng. Commun.*, 2008, **10**, 1803.
16 Y. Kikuchi, Y. Kato, Y. Tanaka, H. Toi and Y. Aoyama, *J. Am. Chem. Soc.*, 1991, **113**, 1349; S. Zheng and P. Coppens, *Chem. Eur. J.,* 2005, **11**, 3583.
17 G. M. Mamardashvili, *Russ. J. Coord. Chem.*, 2006, 10, **756**; A. Mulholland, P. Thordason, E. J. Mensforth and S. Langford, *J. Org. Biomol. Chem.,* 2012, **10**, 6045; O. Middel, W. Verboom and D. N. Reinhoudt, *J. Org. Chem.*, 2001, **66**, 3998.
18 P. Thordarson, *Chem. Soc. Rev.,* 2011, **40**, 1305.